A Centralized Preamble Detection-Based Random Access Scheme for LTE CoMP Transmission

Qiwei Wang, Guangliang Ren, *Member, IEEE*, and Jueying Wu

***Abstract*—For the coordinated multipoint (CoMP) transmission in Long-Term Evolution (LTE) systems, its performance is greatly impacted by the estimation of timing offsets (TOs) between cell-edge user equipment (UE) and transmit points, which is supposed to be dealt with by using the random access (RA) procedure. Available RA schemes for the CoMP transmission offer poor RA performance in terms of multiuser detection, TO estimation, power estimation, and access delays. To improve the RA performance and fully exploit the CoMP structure, in this paper, we propose a novel centralized parallel RA (CP-RA) scheme, which performs in threefold. First, a novel RA subchannel allocation scheme is proposed to suppress mutual interference between coordinated users and noncoordinated users. Second, an iterative parallel interference cancelation (IPIC)-based multiuser detection and estimation algorithm is proposed on the basis of the space-alternating generalized expectation–maximization (SAGE) algorithm. Finally, the coordinated diversity of the system structure could be exploited to implement centralized multiuser detection. Analyses and simulation results show that the proposed RA scheme is able to provide satisfied RA performance compared with existing schemes.**

***Index Terms*—Centralized parallel random access (CP-RA), coordinated diversity, coordinated multipoint (CoMP), frequency-division multiplexed subchannels, iterative parallel interference cancelation (IPIC), Long-Term Evolution (LTE).**

I. Introduction

In Long Term-Evolution (LTE) systems, coordinated multipoint (CoMP) transmission has been recognized as a spectrally efficient technique, with which the geographically distributed transmission points (TPs), particularly E-UTRAN Nodes B (eNodeBs), coordinate to mitigate intercell interference and enhance the transmission of cell-edge user equipment (UE). However, there are many obstacles before it can be put into practical use, and the key one is the estimation of timing offsets (TOs) between coordinated UEs (CoUEs) and distributed TPs [1], [2].

Several research studies have been done for the CoMP transmission with the presence of TOs in [3]–[5], in which implicit assumptions are made that distributed TPs could accurately estimate TOs and that the central unit (CU) has exact knowledge about TOs. A TO compensation scheme is proposed in [3] to replace the conventional timing advance technique to lower the requirement for the length of the cyclic prefix (CP), and two CoMP transmission schemes are proposed to cope with TOs in [4] and [5]. They show that the CoMP transmission could be carried out without performance degradation once the knowledge about TOs is exactly known to the CU. In [6], a TO estimation scheme is performed to alternatively estimate TOs at the UE side for dynamic TP selection. However, it also requires perfect initial TO information and cannot be applied to other CoMP scenarios, e.g., joint processing/transmission or coordinated scheduling/beamforming.

To obtain the knowledge about the TO and power from a UE to its serving eNodeB, in LTE systems, a random access (RA) procedure is utilized for a UE when it: 1) starts an initial access for network entry; 2) goes through a handover process; 3) periodically adjusts the TO information; and 4) requests bandwidth. Moreover, the conventional correlation-based multiuser detection algorithm is utilized to complete the RA procedure [7]–[10]. While for the CoMP transmission, each UE has to complete several RA procedures with all distributed TPs for the CU to obtain the knowledge about TOs and power. By doing so, the TO compensation [3] and the CoMP transmission schemes [4], [5] could be implemented. It is also worth noting that the initial power estimation can be utilized for the TP clustering scheme for further CoMP transmission [11].

Two RA schemes have been proposed for the coordinated transmission [12], [13] on the basis of the aforementioned conventional correlation algorithm. In [12], a distributed serial RA (DS-RA) scheme is utilized for the coordinated carrier aggregation technique, and only one RA procedure is ongoing at any time. This scheme successively accomplishes uplink synchronization of one CoUE with all distributed TPs but at the cost of large access delays, reducing system efficiency. In [13], a distributed parallel RA (DP-RA) scheme is proposed for the coordinated relay network, and one UE initiates the RA procedures with all distributed TPs simultaneously. However, as one CoUE may not establish uplink synchronization with all distributed TPs during one RA procedure, more RA procedures are required for the rest of unsynchronized TPs, thus introducing access delays also. Furthermore, both the DS-RA and DP-RA schemes suffer three problems. The first problem is that the CU is unable to identify both CoUEs and noncoordinated UEs (non-CoUEs) with mutual interference between them. The second problem is that the conventional correlation-based algorithm offers poor multiuser detection and estimation performance

Manuscript received August 21, 2014; revised December 1, 2014 and January 25, 2015; accepted January 31, 2015. Date of publication February 4, 2015; date of current version July 14, 2016. This work was supported in part by the National Natural Science Foundation of China under Grant 61072102, by the National Key Science and Technology Projects of China under Grant 2011ZX03001-007-01, and by the National Key Basic Research Program of China (973 Program) under Grant 2014CB340205. The review of this paper was coordinated by Prof. G. Mao.

The authors are with the State Key Laboratory of Integrated Services Networks, Xidian University, Xi'an 710071, China (e-mail: merling870113@163.com).

Color versions of one or more of the figures in this paper are available online at http://ieeexplore.ieee.org.

Digital Object Identifier 10.1109/TVT.2015.2399503

due to the existence of interference, which results because of the multiple-access interference (MAI) and near–far effect (NFE) among UEs. The last problem is that the coordinated network structure has not been fully exploited to provide certain diversity gain for multiuser detection.

In this paper, aiming at improving the RA performance in terms of multiuser detection, TO estimation, power estimation, and access delays, we propose a centralized parallel RA (CP-RA) scheme for the CoMP transmission as follows.

- First, to facilitate the CU to distinguish CoUEs from non-CoUEs and to suppress mutual interference between them, the signals of CoUEs and non-CoUEs are allocated to different frequency-division multiplexed RA subchannels, whereas in each RA subchannel, the signals of non-CoUEs or CoUEs are still code-division multiplexed.
- Second, aiming at improving the distributed detection and estimation performance in each RA subchannel, a low-complexity iterative parallel interference cancelation (IPIC) algorithm is proposed according to the space-alternating generalized expectation–maximization (SAGE) algorithm [14], which is improved to be applied into this semiblind multiuser detection and estimation scenario.
- Finally, benefitting from the proposed RA subchannel, CoUEs could be easily identified, and their distributed detection metrics could be forwarded to the CU through backhaul links for centralized multiuser detection by exploiting the coordinated diversity of the CoMP structure.

This paper is arranged as follows. Section II introduces the background and signal model of the RA procedure briefly. Section III proposes the RA subchannel allocation scheme, low-complexity IPIC-based multiuser detection algorithm, and the centralized multiuser detection. Simulation parameters and results are shown in Section IV along with the discussion, and the conclusion is presented in Section V.

The following notations are utilized. Matrices and vectors are denoted by symbols in boldface and variables in italic. $\mathbf{1}_{M\times N}$ and $\mathbf{0}_{M\times N}$ stand for $M \times N$ all-one and all-zero matrices. $\mathbf{A} = \mathrm{diag}\{a(n), n = 0, 1, \ldots, N-1\}$ denotes an $N \times N$ diagonal matrix, and $\mathrm{tr}\{\mathbf{B}\}$ represents the trace of a square matrix $\mathbf{B}$. Notations $(\cdot)^T$, $(\cdot)^\dagger$, and $(\cdot)^H$ are used for transpose, conjugate, and Hermitian transposition, respectively. $\lceil x \rceil$ is the smallest integer that is not smaller than x, and $\lfloor x \rfloor$ is the largest integer that is smaller than or equal to x.

II. System and Signal Model

The system model is according to the LTE standard [15], and a diagram of LTE uplink is shown in Fig. 1. In LTE uplink, the physical RA channel (PRACH) is multiplexed with both the physical uplink shared channel (PUSCH) and the physical uplink control channel (PUCCH). As the single-carrier frequency-division multiple-access (SC-FDMA) structure is adopted and there are 14 SC-FDMA symbols with normal CP length in one subframe (i.e., 1 ms) for both the PUSCH

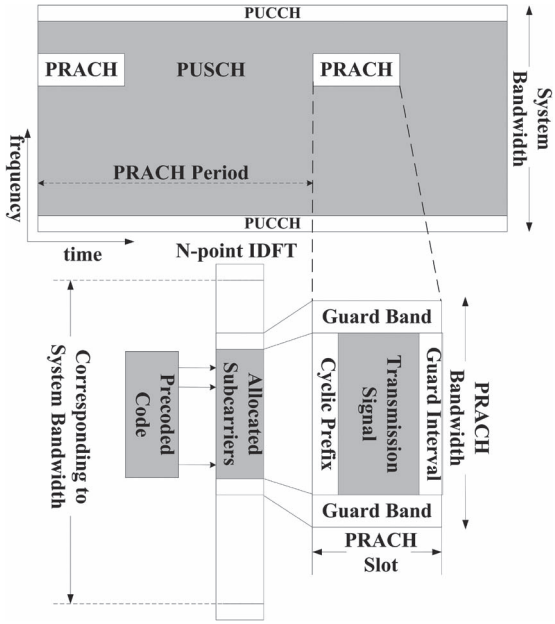

Fig. 1. Illustrative diagram of LTE uplink and PRACH.

and the PUCCH, each symbol consists of $\mathcal{N}$ subcarriers with subcarrier spacing of Δf, whereas the PRACH consists of one SC-FDMA symbol with $N = 12\mathcal{N}$ subcarriers and subcarrier spacing of $\Delta f/12$, lasting for a time duration period of one subframe. This indicates that the PRACH is not orthogonal with the PUSCH and PUCCH, and a filter is then needed to separate them. Therefore, signals of the PUSCH and PUCCH are not considered in what follows. Furthermore, as this paper concentrates on the multiuser detection issues, only a certain PRACH slot is mainly taken into account.

In the PRACH, there are M_t subcarriers corresponding to its bandwidth, in which M continuous subcarriers are allocated to transmit preambles for network entry with the rest of $M_t - M$ subcarriers located at both sides as guard bands. Indexes of allocated subcarriers are defined as $\{\mathcal{K}_m, m = 0, \ldots, M-1\}$, which are regulated by the PRACH configuration index that indicates both the starting subcarrier index and the slot index for the PRACH. According to the PRACH configuration index, for each distributed TP, the time–frequency resources allocated to the PRACH are regulated by the CU. For parallel RA schemes, the PRACH configuration indexes for all distributed TPs must be allocated the same such that signals of CoUEs could be simultaneously received by all distributed TPs. While for the DS-RA scheme, the PRACH configuration indexes could be allocated either the same or not.

To initiate the RA procedure, one UE that tries to access into the network should first establish downlink synchronization with one TP that has the strongest power strength, and this TP acts as its serving TP. The UE obtains the downlink signal-to-interference-plus-noise ratio (SINR) of its serving TP to other neighboring TPs plus noise. If the SINR is large enough, the UE decides itself a non-CoUE and initiates a corresponding RA procedure; otherwise, it decides itself a CoUE. After this, each UE sends a preamble that is randomly selected from a set of discrete Fourier transform (DFT) precoded Zadoff–Chu

(ZC) codes $\mathbb{C} = [\mathbf{C}_1, \ldots, \mathbf{C}_v, \ldots, \mathbf{C}_V]$, and the vth preamble is represented as

$$\mathbf{C}_v = \mathrm{diag}\{\mathcal{C}_v(0), \ldots, \mathcal{C}_v(m), \ldots, \mathcal{C}_v(M-1)\} \quad (1)$$

where $\mathcal{C}_v(m)$ is the mth element of the vth preamble. Assuming that the PRACH is shared by K UEs (including both CoUEs and non-CoUEs) and that the preamble $\mathbf{C}_{v_k}$ is randomly selected by the kth UE, the preamble is then mapped onto allocated subcarriers of the PRACH and processed by an N-point inverse DFT (IDFT) to form the transmission signal as

$$S_{v_k}(n) = \frac{1}{\sqrt{N}} \sum_{m=0}^{M-1} \mathcal{C}_{v_k}(m)\, e^{j2\pi \frac{\mathcal{K}_m}{N} n}, 0 \leqslant n \leqslant N-1. \quad (2)$$

After this, the resulting signal is added with a CP and a guard interval (GI) to occupy a time duration period of one subframe. The time-domain signals of all UEs then propagate through their respective multipath channels and arrive at distributed TPs with corresponding TOs. If there are B TPs in the coordinated region, at the bth TP, the received RA signal, which is an overlap of transmission signals of active UEs, is expressed as

$$y^{(b)}(n) = \sum_{k=1}^{K} \sum_{l=d_{v_k}^{(b)}}^{d_{v_k}^{(b)}+L-1} h_{v_k}^{(b)}\left(l - d_{v_k}^{(b)}\right) S_{v_k}(n-l) + w^{(b)}(n) \quad (3)$$

where $b = 1, \ldots, B$, $d_{v_k}^{(b)}$ and $h_{v_k}^{(b)}(l)$ are the TO and the lth channel tap of the kth UE, the channel impulse response is assumed to have a maximum delay spread of $L-1$ samples such that $h_{v_b}(l) = 0$ for $l < 0$ and $l \geqslant L$, and $w^{(b)}(n)$ accounts for additive white Gaussian noise (AWGN) samples.

The samples of the received signal are transferred into the frequency domain by using an N-point DFT after discarding the CP and GI. At the bth TP, the RA signal in the frequency domain is then extracted from allocated subcarriers as

$$Y^{(b)}(\mathcal{K}_m) = \sum_{k=1}^{K} \mathcal{C}_{v_k}(m) \Phi_m\left(d_{v_k}^{(b)}\right) H_{v_k}^{(b)}(\mathcal{K}_m) + W^{(b)}(\mathcal{K}_m) \quad (4)$$

where $\Phi_m(d_{v_k}^{(b)}) = e^{-j2\pi(\mathcal{K}_m/N)d_{v_k}^{(b)}}$ denotes the phase shift that results because of the TO, $H_{v_k}^{(b)}(\mathcal{K}_m)$ is the channel frequency response (CFR) on the subcarrier $\mathcal{K}_m$, and $W^{(b)}(\mathcal{K}_m)$ represents the AWGN in the frequency domain.

The received signal is represented in the matrix form as

$$\begin{aligned}\mathbf{Y}^{(b)} &= \left[Y^{(b)}(\mathcal{K}_0), \ldots, Y^{(b)}(\mathcal{K}_m), \ldots, Y^{(b)}(\mathcal{K}_{M-1})\right]^T \\ &= \sum_{k=1}^{K} \mathbf{C}_{v_k} \mathbf{F} \mathbf{h}_{v_k}^{(b)} + \mathbf{W}^{(b)} = \sum_{k=1}^{K} \mathbf{C}_{v_k} \mathbf{\Psi}\left(d_{v_k}^{(b)}\right) \mathbf{H}_{v_k}^{(b)} + \mathbf{W}^{(b)}\end{aligned} \quad (5)$$

where $\mathbf{F}$ is an N-point DFT matrix with dimension of $M \times N$, and its entry is given as

$$[\mathbf{F}]_{m,n} = \frac{e^{-j2\pi \frac{\mathcal{K}_m}{N} n}}{\sqrt{N}},\ 0 \leqslant m \leqslant M-1,\ 0 \leqslant n \leqslant N-1 \quad (6)$$

$$\mathbf{h}_{v_k}^{(b)} = \left[\mathbf{0}_{1\times d_{v_k}^{(b)}} \quad \boldsymbol{\xi}_{v_k}^{(b)} \quad \mathbf{0}_{1\times\left(N-L-d_{v_k}^{(b)}\right)}\right]^T \quad (7)$$

$$\boldsymbol{\xi}_{v_k}^{(b)} = \left[h_{v_k}^{(b)}(0), \ldots, h_{v_k}^{(b)}(l), \ldots, h_{v_k}^{(b)}(L-1)\right] \quad (8)$$

$$\mathbf{\Psi}\left(d_{v_k}^{(b)}\right) = \mathrm{diag}\left\{\Phi_m\left(d_{v_k}^{(b)}\right),\ 0 \leqslant m \leqslant M-1\right\} \quad (9)$$

$$\mathbf{H}_{v_k}^{(b)} = \left[H_{v_k}^{(b)}(\mathcal{K}_0), \ldots, H_{v_k}^{(b)}(\mathcal{K}_m), \ldots, H_{v_k}^{(b)}(\mathcal{K}_{M-1})\right]^T \quad (10)$$

$$\mathbf{W}^{(b)} = \left[W^{(b)}(\mathcal{K}_0), \ldots, W^{(b)}(\mathcal{K}_m), \ldots, W^{(b)}(\mathcal{K}_{M-1})\right]^T. \quad (11)$$

In this paper, possible collisions in the multiuser detection stage are neglected. This is because, after the multiuser detection stage, possible collisions could be detected by a scheduled transmission through which each UE that is corresponding to a detected code should send its device identification on allocated resources in the PUSCH [16]. In case a collision happens, colliding UEs would send their device identifications on the same resources so that the CU is unable to identify them, and these UEs should reinitiate new RA processes.

III. Proposed Centralized Parallel Random Access Scheme for Coordinated Multipoint Transmission

Here, a novel RA subchannel allocation scheme is first proposed. After this, a low-complexity IPIC-based distributed multiuser detection and estimation algorithm is proposed to suppress interference, which results because of MAI and NFE in each RA subchannel, and some issues in detail for the proposed IPIC algorithm are also discussed. Finally, based on the proposed subchannel allocation scheme and the IPIC algorithm, the centralized detection is performed for CoUEs by exploiting the coordinated diversity.

A. Problem in Conventional PRACH

Here, the problem of the correlation-based multiuser detection algorithm in the conventional PRACH is illustrated, and impacts of the NFE and MAI are depicted.

The conventional correlation-based multiuser detection algorithm is discussed in [7]–[10], in which the correlation process is actually implemented to derive the transform-domain channel taps because 1) ZC codes should be decoded into the transform domain by using an M-point IDFT, 2) the cyclic shift of ZC codes facilitates the channel estimation, and 3) an M-point IDFT could significantly reduce the computational complexity instead of an N-point IDFT. The correlation-based algorithm is given in the Appendix, in which the vector of transform-domain channel taps of a code $\mathbf{C}_{v_k}$ is defined as

$$\begin{aligned}\boldsymbol{g}_{v_k}^{(b)} &= \left[g_{v_k}^{(b)}(0), \ldots, g_{v_k}^{(b)}(\ell), \ldots, g_{v_k}^{(b)}(M-1)\right]^T \\ &= \frac{1}{M}\mathbf{Q}^H \mathbf{\Psi}\left(d_{v_k}^{(b)}\right) \mathbf{H}_{v_k}^{(b)} = \frac{1}{M}\mathbf{Q}^H \mathbf{F} \mathbf{h}_{v_k}^{(b)}\end{aligned} \quad (12)$$

and $\mathbf{Q}$ is an M-point DFT matrix with its entry given as

$$[\mathbf{Q}]_{m,\ell} = \frac{e^{-j2\pi\frac{m}{M}\ell}}{\sqrt{M}},\ 0 \leqslant m \leqslant M-1,\ 0 \leqslant \ell \leqslant M-1. \tag{13}$$

According to the estimation of $\boldsymbol{g}_{v_k}^{(b)}$, the activity of the current code could be determined, and its parameters, including the TO and power, could be estimated.

Assume that the PRACH is shared by K_c CoUEs with indexes of $\{v_k, k = 1, 2, \ldots, K_c\}$ and K_n non-CoUEs with indexes of $\{u_k, k = 1, 2, \ldots, K_n\}$, where $K_n + K_c = K$. Without loss of generality, the first CoUE is considered for example. As the correlation-based algorithm is proceeded for each possible code by treating other active codes as interference, its transform-domain channel taps could be estimated as

$$\begin{aligned}\widehat{\boldsymbol{g}}_{v_1}^{(b)} &= \frac{1}{M}\mathbf{Q}^H\mathbf{C}_{v_1}^H\mathbf{Y}^{(b)} = \boldsymbol{g}_{v_1}^{(b)} + \frac{1}{M}\mathbf{Q}^H\mathbf{C}_{v_1}^H\mathbf{W}^{(b)} \\ &+ \underbrace{\frac{1}{M}\mathbf{Q}^H\mathbf{C}_{v_1}^H\sum_{k=2}^{K_c}\mathbf{C}_{v_k}\mathbf{F}\mathbf{h}_{v_k}^{(b)}}_{\text{Interference from other CoUEs}} + \underbrace{\frac{1}{M}\mathbf{Q}^H\mathbf{C}_{v_1}^H\sum_{k=1}^{K_n}\mathbf{C}_{u_k}\mathbf{F}\mathbf{h}_{u_k}^{(b)}}_{\text{Interference from non-CoUEs}}.\end{aligned} \tag{14}$$

It is obviously shown that the channel estimation of the current CoUE is greatly impacted by signals of other CoUEs and non-CoUEs, and the interference exists due to the following two reasons. 1) On one hand, according to LTE standards [15], [16], initial power control and power ramping mechanisms are employed to compensate the path loss (PL). However, as CoUEs are distributed over cell borders with large PLs, it is possible that the PL of a CoUE to a distributed TP cannot be fully compensated although the maximum transmitting power is reached. The receiving power would be further fluctuated by shadow fading, small-scale fading, estimation errors of PLs, and power ramping, etc. In addition, if a parallel RA scheme is utilized, one CoUE could only adjust its transmitting power toward one of the distributed TPs, leaving the PLs to other TPs not fully compensated or overcompensated. Hence, the NFE always exists among UEs. 2) On the other hand, due to the existence of frequency-selective channels and TOs, the orthogonality of ZC codes is damaged, and the detection of the current preamble is thus impacted by other active codes, introducing great MAI among UEs, particularly when there is a large number of UEs.

B. Proposed RA Subchannel Allocation Scheme

To suppress mutual interference between CoUEs and non-CoUEs and facilitate the CU to identify CoUEs for centralized detection, we divide the PRACH into frequency-division multiplexed RA subchannels, by which more RA opportunities (one RA opportunity is a preamble in one PRACH) could be also provided than the conventional PRACH. Defining the number of subcarriers of subchannels for CoUEs and non-CoUEs as M_c and M_n, respectively, and the number of subcarriers for the guard band between subchannels as M_g, we consider the following guidelines: 1) $M_c + M_n + M_g = M$, 2) M_c and M_n should be prime numbers to guarantee maximum numbers of root ZC sequences, and 3) M_c and M_n should be chosen as great as possible to guarantee the length of ZC codes for TO estimation.

Without loss of generality, we only consider the RA subchannel for CoUEs, and the analysis for non-CoUEs is quite similar. Subcarrier indexes in the RA subchannel are defined as $\{\mathcal{J}_m,\ m = 0, \ldots, M_c - 1\} \subset \{\mathcal{K}_m, m = 0, \ldots, M-1\}$. To compare the RA subchannel with the conventional PRACH, the following conditions are assumed to be consistent with that in (5) for each CoUE, i.e., the signal propagates through the same multipath channel, the PL is the same such that the transmitting power is constant, and the AWGN is also the same. The received signal in the RA subchannel is given as

$$\begin{aligned}\overline{\mathbf{Y}}^{(b)} &= \left[\overline{Y}^{(b)}(\mathcal{J}_0), \ldots, \overline{Y}^{(b)}(\mathcal{J}_m), \ldots, \overline{Y}^{(b)}(\mathcal{J}_{M_c-1})\right]^T \\ &= \sqrt{\frac{M}{M_c}}\sum_{k=1}^{K_c}\overline{\mathbf{C}}_{v_k}\overline{\mathbf{\Psi}}\left(d_{v_k}^{(b)}\right)\overline{\mathbf{H}}_{v_k}^{(b)} + \overline{\mathbf{W}}^{(b)} \\ &= \sqrt{\frac{M}{M_c}}\sum_{k=1}^{K_c}\overline{\mathbf{C}}_{v_k}\overline{\mathbf{F}}\mathbf{h}_{v_k}^{(b)} + \overline{\mathbf{W}}^{(b)}\end{aligned} \tag{15}$$

where $\overline{\mathbf{C}}_{v_k}$ is a precoded ZC code designed for the RA subchannel with its length being M_c; $\sqrt{M/M_c}$ is the amplitude amplification factor due to constant transmitting power and less number of subcarriers compared with that in (5); and matrices $\overline{\mathbf{F}}$, $\overline{\mathbf{\Psi}}(d_{v_k}^{(b)})$, $\overline{\mathbf{H}}_{v_k}^{(b)}$, and $\overline{\mathbf{W}}^{(b)}$ are the $M_c \times N$ DFT matrix, the phase-shift matrix, the CFR, and the frequency-domain AWGN corresponding to subcarriers $\{\mathcal{J}_m, m = 0, \ldots, M_c - 1\}$, respectively.

As the number of subcarriers in the RA subchannel is M_c, an M_c-point IDFT is utilized to obtain the transform-domain channel taps, which is defined as

$$\begin{aligned}\overline{\boldsymbol{g}}_{v_k}^{(b)} &= \left[\overline{g}_{v_k}^{(b)}(0), \ldots, \overline{g}_{v_k}^{(b)}(\ell), \ldots, \overline{g}_{v_k}^{(b)}(M_c-1)\right]^T \\ &= \frac{1}{M_c}\overline{\mathbf{Q}}^H\overline{\mathbf{\Psi}}\left(d_v^{(b)}\right)\overline{\mathbf{H}}_{v_k}^{(b)} = \frac{1}{M_c}\overline{\mathbf{Q}}^H\overline{\mathbf{F}}\mathbf{h}_{v_k}^{(b)}\end{aligned} \tag{16}$$

where $\overline{\mathbf{Q}}$ is an M_c-point DFT matrix with its entry given as

$$[\overline{\mathbf{Q}}]_{m,\ell} = \frac{e^{-j2\pi\frac{m}{M_c}\ell}}{\sqrt{M_c}},\ 0 \leqslant m \leqslant M_c-1,\ 0 \leqslant \ell \leqslant M_c-1. \tag{17}$$

To compare with the channel estimation in (14), the received signal in (15) is first normalized by dividing the amplitude amplification factor, and the transform-domain channel estimation is then derived as

$$\begin{aligned}\widehat{\overline{\boldsymbol{g}}}_{v_1}^{(b)} &= \frac{1}{M_c}\overline{\mathbf{Q}}^H\overline{\mathbf{C}}_{v_1}{}^H\overline{\mathbf{Y}}^{(b)} = \overline{\boldsymbol{g}}_{v_1}^{(b)} + \sqrt{\frac{1}{MM_c}}\overline{\mathbf{Q}}^H\overline{\mathbf{C}}_{v_1}^H\overline{\mathbf{W}}^{(b)} \\ &+ \underbrace{\sqrt{\frac{1}{MM_c}}\overline{\mathbf{Q}}^H\overline{\mathbf{C}}_{v_1}^H\sum_{k=2}^{K_c}\overline{\mathbf{C}}_{v_k}\overline{\mathbf{F}}\mathbf{h}_{v_k}^{(b)}}_{\text{Interference from other CoUEs}}.\end{aligned} \tag{18}$$

Note that $\overline{\mathbf{F}}$ and $\overline{\mathbf{W}}^{(b)}$ are actually a part of $\mathbf{F}$ and $\mathbf{W}^{(b)}$, respectively. As both $\mathbf{h}_{v_k}^{(b)}$ and $\mathbf{W}^{(b)}$ follow complex Gaussian distribution with zero mean, both $\widehat{\boldsymbol{g}}_{v_1}^{(b)}$ and $\widehat{\overline{\boldsymbol{g}}}_{v_1}^{(b)}$ could be deemed as complex Gaussian variables with mean values of $\boldsymbol{g}_{v_1}^{(b)}$ and $\overline{\boldsymbol{g}}_{v_1}^{(b)}$, respectively, indicating that $\widehat{\boldsymbol{g}}_{v_1}^{(b)}$ and $\widehat{\overline{\boldsymbol{g}}}_{v_1}^{(b)}$ are unbiased estimations.

Assuming that the covariance matrices of $\mathbf{h}_{v_k}^{(b)}$, $\mathbf{W}^{(b)}$, and $\overline{\mathbf{W}}^{(b)}$ are $\mathbf{V}_{\mathbf{h}_{v_k}^{(b)}} = E\{\mathbf{h}_{v_k}^{(b)}\mathbf{h}_{v_k}^{(b)H}\}$, $\mathbf{V}_{\mathbf{W}^{(b)}} = \sigma_W^2\mathbf{I}_M$, and $\mathbf{V}_{\overline{\mathbf{W}}^{(b)}} = \sigma_W^2\mathbf{I}_{M_c}$, respectively, the mean square errors (MSEs) of both channel estimates could be represented as

$$\begin{aligned} E\left\{\left\|\widehat{\boldsymbol{g}}_{v_1}^{(b)} - \boldsymbol{g}_{v_1}^{(b)}\right\|^2\right\} &= \frac{1}{M}\sigma_W^2 + \frac{1}{M^2}\sum_{k=2}^{K_c}\mathrm{tr}\left\{\mathbf{F}^H\mathbf{F}\mathbf{V}_{\mathbf{h}_{v_k}^{(b)}}\right\} \\ &\quad + \frac{1}{M^2}\sum_{k=1}^{K_n}\mathrm{tr}\left\{\mathbf{F}^H\mathbf{F}\mathbf{V}_{\mathbf{h}_{u_k}^{(b)}}\right\} \\ &= \frac{1}{M}\sigma_W^2 + \frac{1}{MN}\sum_{k=2}^{K_c}P_{\mathbf{h}_{v_k}^{(b)}} + \frac{1}{MN}\sum_{k=1}^{K_n}P_{\mathbf{h}_{u_k}^{(b)}} \end{aligned} \tag{19}$$

$$\begin{aligned} E\left\{\left\|\widehat{\overline{\boldsymbol{g}}}_{v_1}^{(b)} - \overline{\boldsymbol{g}}_{v_1}^{(b)}\right\|^2\right\} &= \frac{1}{M}\sigma_W^2 + \frac{1}{MM_c}\sum_{k=2}^{K_c}\mathrm{tr}\left\{\overline{\mathbf{F}}^H\overline{\mathbf{F}}\mathbf{V}_{\mathbf{h}_{v_k}^{(b)}}\right\} \\ &= \frac{1}{M}\sigma_W^2 + \frac{1}{MN}\sum_{k=2}^{K_c}P_{\mathbf{h}_{v_k}^{(b)}} \end{aligned} \tag{20}$$

where

$$P_{\mathbf{h}_{v_k}^{(b)}} = \mathrm{tr}\left\{\mathbf{V}_{\mathbf{h}_{v_k}^{(b)}}\right\} = E\left\{\mathbf{h}_{v_k}^{(b)H}\mathbf{h}_{v_k}^{(b)}\right\}. \tag{21}$$

When deriving (19) and (20), two facts are utilized, i.e., 1) diagonal elements of $\mathbf{F}^H\mathbf{F}$ and $\overline{\mathbf{F}}^H\overline{\mathbf{F}}$ are equal to M/N and M_c/N, respectively, and 2) $\mathbf{V}_{\mathbf{h}_{v_k}^{(b)}}$ is a diagonal matrix.

Inspection of (19) and (20) shows that the channel estimation in the conventional PRACH suffers interference from both CoUEs and non-CoUEs, and the utilization of the proposed RA subchannels is able to mitigate mutual interference between CoUEs and non-CoUEs. Since the multiuser detection and estimation performance mainly depends on the channel estimation results, more accurate channel estimation results could be provided by the RA subchannel, leading to better performance. In addition, it is worth noting that the performance of TO estimation would be impacted by the proposed RA subchannels. The expression of TO estimation is given in (36) in the Appendix, and it can be found that the accuracy of TO estimation relates to the number of subcarriers. With other conditions being the same, less number of subcarriers leads to worse TO estimation performance, which explains why the third guideline in designing the RA subchannels is required. However, by mitigating interference in each RA subchannel and utilizing an effective multiuser detection and estimation algorithm, on the contrary, the accuracy of TO estimation could be improved instead.

C. Low-Complexity IPIC Algorithm for Distributed Multiuser Detection and Estimation

Although interference between CoUEs and non-CoUEs has been mitigated by using the proposed RA subchannels, it is shown in (20) that interference in each subchannel still exists. To deal with this problem, an IPIC-based multiuser detection algorithm is proposed within the framework of the SAGE algorithm [14], which is able to decompose a complicated maximum-likelihood (ML) problem into several simpler problems by iteratively alternating between an E-step, calculating the log-likelihood function of the complete data, and an M-step, maximizing the expectation with respect to desired parameters.

Without loss of generality, the RA subchannel for CoUEs is still taken into account, and the derivations for non-CoUEs are similar. As the activities of preambles are blind to the TP, the received signal model could be regarded as a linear combination of all possible codes. According to (15), the received signal in the RA subchannel could be modified as

$$\overline{\mathbf{Y}}^{(b)} = \sum_{v=1}^{V}\overline{\mathbf{C}}_v\overline{\boldsymbol{\Psi}}\left(d_v^{(b)}\right)\overline{\mathbf{H}}_v^{(b)} + \overline{\mathbf{W}}^{(b)} \tag{22}$$

where the amplitude amplification factor in (15) has been incorporated into $\overline{\mathbf{H}}_v^{(b)}$, and $\overline{\mathbf{H}}_v^{(b)} = \mathbf{0}_{M_c\times 1}$ if the vth code is inactive. The proposed IPIC algorithm proceeds in such a way that the detection and estimation of each possible code are implemented and updated at a time. This leads to that the proposed IPIC algorithm consists of *iterations* and *stages*, and V stages make an iteration with one possible code detected and estimated in one stage. The estimates of parameters are updated over iterations, and the process continues until no significant changes are observed.

According to the terminology of the SAGE algorithm, the received signal $\overline{\mathbf{Y}}^{(b)}$ is viewed as the observed signal, and the signal of each possible code is deemed as the complete data, i.e., $\mathbf{Z}_v^{(b)} = \overline{\mathbf{C}}_v\overline{\boldsymbol{\Psi}}(d_v^{(b)})\overline{\mathbf{H}}_v^{(b)}$. To avoid error propagation, the detection order of preambles should be arranged from strong to weak. At the ith iteration, the code indexes are reordered as $\{v_\alpha^{(i)}, \alpha = 1, 2, \ldots, V\}$ by rearranging the estimated power of all possible codes in a descend order, and the reconstructed frequency signal of the code $\overline{\mathbf{C}}_{v_\alpha^{(i)}}$ is defined as $\widehat{\mathbf{Z}}_{v_\alpha^{(i)}}^{(b)(i)}$.

The IPIC is initialized by setting the iteration number $i = 0$, and $\widehat{\mathbf{Z}}_{v_\alpha^{(1)}}^{(b)(0)} = \mathbf{0}_{M_c\times 1}$. The E-step and M-step of the IPIC algorithm are subsequently presented.

E-Step: At the ith iteration, compute

$$\begin{aligned} \overline{\mathbf{Y}}_{v_\alpha^{(i)}}^{(b)(i)} &= \overline{\mathbf{Y}}^{(b)} - \sum_{\beta=1}^{\alpha-1}\widehat{\mathbf{Z}}_{v_\beta^{(i)}}^{(b)(i)} - \sum_{\beta=\alpha+1}^{V}\widehat{\mathbf{Z}}_{v_\beta^{(i)}}^{(b)(i-1)} \\ &= \mathbf{Z}_{v_\alpha^{(i)}}^{(b)} + \boldsymbol{\eta}_{v_\alpha^{(i)}}^{(b)(i)} \end{aligned} \tag{23}$$

where

$$\begin{aligned} \boldsymbol{\eta}_{v_\alpha^{(i)}}^{(b)(i)} &= \sum_{\beta=1}^{\alpha-1}\left[\mathbf{Z}_{v_\beta^{(i)}}^{(b)} - \widehat{\mathbf{Z}}_{v_\beta^{(i)}}^{(b)(i)}\right] + \overline{\mathbf{W}}^{(b)} \\ &\quad + \sum_{\beta=\alpha+1}^{V}\left[\mathbf{Z}_{v_\beta^{(i)}}^{(b)} - \widehat{\mathbf{Z}}_{v_\beta^{(i)}}^{(b)(i-1)}\right]. \end{aligned} \tag{24}$$

Note that $\boldsymbol{\eta}_{v_\alpha^{(i)}}^{(b)(i)}$ is a disturbance term that consists of AWGN and residual interference added to the code $\overline{\mathbf{C}}_{v_\alpha^{(i)}}$ at the ith iteration, and entries of $\boldsymbol{\eta}_{v_\alpha^{(i)}}^{(b)(i)}$ are nearly complex Gaussian distributed with zero mean [14], [18].

M-Step: Compute

$$\widehat{\mathbf{Z}}_{v_\alpha^{(i)}}^{(b)(i)} = \arg\min \left\| \overline{\mathbf{Y}}_{v_\alpha^{(i)}}^{(b)(i)} - \mathbf{Z}_{v_\alpha^{(i)}}^{(b)} \right\|^2. \tag{25}$$

It is shown that the complicated ML problem can be split into V simpler problems by using the SAGE algorithm. The M-Step could be solved by using the least square (LS) estimation in (16), which is re-expressed as

$$\begin{aligned}\widehat{\boldsymbol{g}}_{v_\alpha^{(i)}}^{(b)(i)} &= \frac{1}{M_c}\overline{\mathbf{Q}}^H \overline{\mathbf{C}}_{v_\alpha^{(i)}}^H \overline{\mathbf{Y}}_{v_\alpha^{(i)}}^{(b)(i)} = \frac{1}{M_c}\overline{\mathbf{Q}}^H \overline{\mathbf{C}}_{v_\alpha^{(i)}}^H \left[\mathbf{Z}_{v_\alpha^{(i)}}^{(b)} + \boldsymbol{\eta}_{v_\alpha^{(i)}}^{(b)(i)}\right] \\ &= \frac{1}{M_c}\left[\overline{\mathbf{Q}}^H \overline{\boldsymbol{\Psi}}\left(d_{v_\alpha^{(i)}}^{(b)}\right)\overline{\mathbf{H}}_{v_\alpha^{(i)}}^{(b)} + \overline{\mathbf{Q}}^H \overline{\mathbf{C}}_{v_\alpha^{(i)}}^H \boldsymbol{\eta}_{v_\alpha^{(i)}}^{(b)(i)}\right].\end{aligned} \tag{26}$$

Noting that the possible TO of a CoUE $d_{v_k}^{(b)}$ is in the range of $[d_{\min}, d_{\max}]$, which corresponds to the cell radius, CoMP scenario, and sampling rate, the variance of the disturbance item for the current code is estimated as

$$\widehat{\sigma}_{v_\alpha^{(i)}}^{(b)(i)2} = \frac{1}{N_{\rm cs} - D_{\max} - 1} \sum_{\ell = D_{\max}+1}^{N_{\rm cs}-1} \left| \widehat{g}_{v_\alpha^{(i)}}^{(b)(i)}(\ell) \right|^2 \tag{27}$$

where $D_{\max} = \lceil (d_{\max} + L - 1)M_c/N \rceil < N_{\rm cs} - 1$ is defined as the maximum delay spread of the transform-domain channel taps corresponding to that of the time-domain channel taps with a scaler factor M_c/N according to the SC-FDMA structure [19]. Since ZC codes are actually generated as cyclic-shift versions of one root ZC sequence in the transform domain before DFT precoding, defining by $N_{\rm cs}$ the length of cyclic shift of ZC codes, if $\ell \geq N_{\rm cs}$, the current ZC code becomes another one, indicating that only the channel estimates with indexes $\ell \in [0, N_{\rm cs} - 1]$ could be utilized. Therefore, $\ell \in [D_{\max} + 1, N_{\rm cs} - 1]$ is the region for estimating the variance of the disturbance item. Defining $D_{\min} = \lfloor d_{\min} M_c/N \rfloor$ as the minimum TO of a CoUE in the transform domain, for the current code, the detection metric and estimates of the TO and power are then determined as

$$\Upsilon_{v_\alpha^{(i)}}^{(b)(i)} = \max_{\ell \in [D_{\min}, D_{\max}]} \frac{1}{\widehat{\sigma}_{v_\alpha^{(i)}}^{(b)(i)}} \left| \widehat{g}_{v_\alpha^{(i)}}^{(b)(i)}(\ell) \right| \tag{28}$$

$$\widehat{d}_{v_\alpha^{(i)}}^{(b)(i)} = \frac{N}{M_c} \cdot \arg\max_{\ell \in [D_{\min}, D_{\max}]} \frac{1}{\widehat{\sigma}_{v_\alpha^{(i)}}^{(b)(i)}} \left| \widehat{g}_{v_\alpha^{(i)}}^{(b)(i)}(\ell) \right| \tag{29}$$

$$\widehat{P}_{v_\alpha^{(i)}}^{(b)(i)} = \sum_{\ell=0}^{D_{\max}} \left| \widehat{g}_{v_\alpha^{(i)}}^{(b)(i)}(\ell) \right|^2. \tag{30}$$

Defining by λ a predefined detection threshold, the frequency signal of the current code could be reconstructed as

$$\begin{cases} \widehat{\mathbf{Z}}_{v_\alpha^{(i)}}^{(b)(i)} = \overline{\mathbf{C}}_{v_\alpha^{(i)}} \overline{\mathbf{Q}} \mathbf{G} \widehat{\boldsymbol{g}}_{v_\alpha^{(i)}}^{(b)(i)}, & \text{if } \Upsilon_{v_\alpha^{(i)}}^{(b)(i)} \geq \lambda \\ \widehat{\mathbf{Z}}_{v_\alpha^{(i)}}^{(b)(i)} = \mathbf{0}_{M_c \times 1}, & \text{if } \Upsilon_{v_\alpha^{(i)}}^{(b)(i)} < \lambda \end{cases} \tag{31}$$

where $\mathbf{G} = \mathrm{diag}\{\mathbf{1}_{1\times N_{\rm cs}}\ \mathbf{0}_{1\times M_c - N_{\rm cs}}\}$ is a weighting matrix, which is introduced to obtain channel estimates with indexes of $\ell \in [0, N_{\rm cs} - 1]$. Note that most power of channel taps in the transform domain mainly concentrates in the interval $\ell \in [0, N_{\rm cs} - 1]$ according to the SC-FDMA structure [19], which ensures the reconstruction of the frequency signal.

At the end of each iteration, the code indexes should be reordered by rearranging the estimated power of all possible codes in descend according to (30), and the M-Step is actually implemented according to (26)–(31). The IPIC algorithm then alternates between the E-Step and M-Step over iterations until a predefined terminating condition is satisfied.

D. Remarks

1) Intuitively speaking, the IPIC should stop when there is no significant variation observed in the log-likelihood function. To reduce complexity, a simpler stopping criterion is to terminate the IPIC after a predesigned number of iterations $i_{\max}$, which should be further analyzed via simulation results. When the IPIC terminates, the detection metric and estimates of the TO and power of the vth code are eventually given as $\Upsilon_v^{(b)}$, $\widehat{d}_v^{(b)}$, and $\widehat{P}_v^{(b)}$ according to the estimation results in (29) and (30) at the last iteration, i.e., $\Upsilon_v^{(b)(i_{\max})}$, $\widehat{d}_v^{(b)(i_{\max})}$, and $\widehat{P}_v^{(b)(i_{\max})}$.

2) It is known that the initialization of the SAGE algorithm is of great importance. However, in the PRACH, there is no additional information to assist the IPIC into an initialization. Therefore, the IPIC is actually initialized by reordering the code indexes according to the estimated power of all possible codes, which is obtained by using the conventional correlation algorithm that is presented in the Appendix. After this, the detection and estimation for all possible codes could be considered in an order from strong to weak, and the despreading gain of ZC codes is properly guaranteed, along with both the detection threshold and the SAGE algorithm, leading to superior detection and estimation performance.

3) The predefined threshold λ is designed to make a constant false-alarm rate detection. As the disturbance term is nearly complex Gaussian distributed, if a code is invalid, the detection metric in (28) could be deemed as a normalized Rayleigh distributed variable. A false alarm occurs when the detection metric exceeds the threshold that is given as $\lambda = \mathcal{F}_{\rm Ray}^{-1}(1 - P_{\rm fa})$, where $\mathcal{F}_{\rm Ray}^{-1}(\cdot)$ is defined as the inverse cumulative distribution function (CDF) of a normalized Rayleigh variable, and $P_{\rm fa}$ is the desired false-alarm rate. This threshold could be also applied to the conventional correlation algorithm.

4) The computational burden of the proposed IPIC algorithm mainly comes from an initialization and multiuser detection over iterations. The comparison of complexities of both the IPIC and the correlation algorithm in the RA subchannel is given in Table I and would be further analyzed by simulation results in Section IV.

E. Centralized Detection Exploiting Coordinated Diversity

After the detection of CoUEs at distributed TPs, detection metrics and estimated parameters are forwarded to the CU via

TABLE I
COMPLEXITY

	IPIC algorithm	Correlation algorithm
real multiplications	$4VM_cN_{cs} + i_{\max}\left[4VM_cN_{cs} + 4KM_cN_{cs}\right]$	$4VM_cN_{cs}$
real additions	$2VM_c(N_{cs}-1) + i_{\max}\left[2VM_c(N_{cs}-1) + 2KM_c(N_{cs}-1)\right]$	$2VM_c(N_{cs}-1)$

backhaul links. The centralized detection metric exploiting the coordinated diversity for the vth code is designed as

$$\Lambda_v = \sum_{b=1}^{B} \left|\Upsilon_v^{(b)}\right|^2. \tag{32}$$

As previously stated, the distributed detection metric $\Upsilon_v^{(b)}$ is assumed to follow normalized Rayleigh distribution such that the centralized detection metric could be deemed as a chi-square distribution variable with $2B$ degree of freedom and variance of 1/2. In addition, since the channel fading from one CoUE to all distributed TPs is independent, the centralized detection metric is supposed to obtain certain diversity gain, which is named *coordinated diversity*.

Another predesigned threshold γ should be utilized for the centralized detection to guarantee a low level of false-alarm rate. If the vth code is invalid, a false alarm occurs when $\Lambda_v > \gamma$, which is given as $\gamma = \mathcal{F}_{\text{Chi}}^{-1}(1 - P_{\text{fa}}, 2B, 1/2)$, where $\mathcal{F}_{\text{Chi}}^{-1}(1 - P_{\text{fa}}, 2B, 1/2)$ is the inverse CDF of a normalized chi-square variable at the probability of $(1 - P_{\text{fa}})$.

IV. Simulation Results

A. Simulation Parameters

Simulation parameters are chosen in compliance with LTE systems [15], [16] and are presented in Table II. As the Doppler frequency can be estimated and tracked in downlink [20], we assume that the Doppler frequency is preadjusted and only takes into account the residual carrier frequency offset that is less than 2% of the subcarrier spacing. For the proposed CP-RA scheme, according to the guidelines in designing RA subchannels, without loss of generality, the number of subcarriers of the subchannel for CoUEs is selected as 409 and that for non-CoUEs as 419. In this case, 12 and 13 subcarriers are placed on both sides of the PRACH as guard bands and 11 subcarriers as the guard band between RA subchannels. The preambles for the proposed RA subchannel are generated from three root ZC sequences with the length of cyclic shift being 22. For the DS-RA and DP-RA schemes, the conventional PRACH is utilized with 839 subcarriers, and the preambles are generated from two root ZC sequences with the length of the cyclic shift being 22. The conventional correlation algorithm is employed by the DS-RA and DP-RA schemes for comparison.

A general CoMP scenario [21], [22] is utilized, as shown in Fig. 2, where the shadow area stands for the coordinated region, and three eNodeBs are serving as distributed TPs with six sectors in each cell. Without loss of generality and for simplicity, we assume that one UE is a CoUE if its TO (i.e., round-trip delay) exceeds $d_{\min} = 100$ samples; corresponding to this, the minimum distance from a CoUE to its serving TPs is $\Omega_{\min} = d_{\min}c/2f_s = 0.98$ km, with c standing for the speed of light. The maximum distance from a CoUE to its serving TPs is $\Omega_{\max} = 2.28$ km with the maximum TO being $d_{\max} = 233$ samples. In this case, the TO range of non-CoUEs is [0, 100] samples and that of CoUEs is [101, 233] samples.

TABLE II
SIMULATION PARAMETERS

FFT size	12288
CP size	1584
Sampling rate f_s	$15.36MHz$
Subcarrier spacing	$1.25kHz$
Carrier frequency f_c	$2.3GHz$
Cell radius	$1.5km$
Number of preambles	54
Maximum Doppler frequency	$127.8Hz$
Carrier frequency offset	Less than 2%
Standard shadow derivation	$6dB$
Receiving gain G	$6dB$
Noise figure N_f	$4dB$
Maximum transmitting power	$24dBm$
Power ramping step	$2dB$
Channel model	ITU-R M.1225 Veh-A
Vehicle speed	Less than $60km/h$
Noise power spectrum density N_0	$-174dBm/Hz$
Poisson arrival rate of non-CoUEs	5 per RA frame

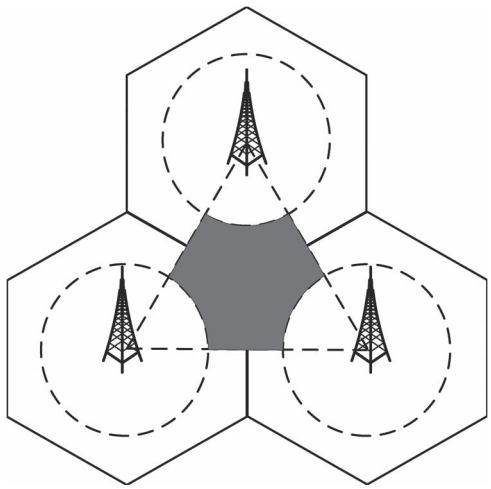

Fig. 2. Sketch of a general CoMP scenario.

To realize the initial power control mechanism, we assume that the PL is ideally obtained in downlink. The PL is applied according to the Okumura–Hata model that is given as $\text{PL}(\Omega) = 128.1 + 37.6 \cdot \log_{10}(\Omega)$, where Ω is the distance from a UE to its serving TP with unit in kilometers. As the total noise power is $\sigma_n^2 = f_s N_0 = -102.14$ dBm, we assume that the target receiving power is the same as the noise power, i.e., $P_r = -102.14$ dBm, and the transmitting power of a UE is then adjusted as $P_t(\Omega) = P_r + \text{PL}(\Omega) - G - N_f$. The initial power control for the RA schemes is described as follows.

- **CP-RA scheme**: 1) For non-CoUEs, since $\Omega_{\min}$ is the maximum distance from non-CoUEs to their serving TPs, we have $P_t(\Omega_{\min}) = 15.63$ dBm $< P_{t,\max} = 24$ dBm, which means that the PLs of non-CoUEs can be completely compensated. Since the bandwidth of the RA subchannel for non-CoUEs is 523.75 kHz, corresponding to which the noise power is -116.81 dBm, the SNR of non-CoUEs is 14.67 dB. 2) For CoUEs, when the transmitting power reaches the maximum transmitting power, to achieve the target receiving power, the maximum distance from CoUEs to distributed TPs is obtained as 1.64 km $< \Omega_{\max}$, indicating that, if a CoUE is too far away from a TP, its PL cannot be fully compensated. Corresponding to the serving TP, the minimum receiving power of a CoUE is then obtained as -107.56 dBm. As the bandwidth of the RA subchannel for CoUEs is 511.25 kHz, corresponding to which the noise power is -116.91 dBm, the SNR of CoUEs resides in the range [9.35, 14.77] dB.
- **DP-RA and DS-RA schemes**: As the conventional PRACH is utilized for DP-RA and DS-RA schemes, its bandwidth is 104.875 kHz, corresponding to which the noise power is -113.79 dBm. 1) For non-CoUEs, their PLs could be fully compensated, and the SNR of non-CoUEs is 11.65 dB. 2) For CoUEs, when the transmitting power achieves the maximum, corresponding to a certain TP, the minimum receiving power is -107.56 dBm, and the SNR of CoUEs is in the range [6.23, 11.65] dB.

Note that the SNR of both CoUEs and non-CoUEs would be further impacted by shadow fading, small-scale fading, and power ramping. It is worth mentioning that, for parallel RA schemes (i.e., CP-RA and DP-RA schemes), the transmitting power of a CoUE is adjusted according to the minimum PL to alleviate the NFE, which would further fluctuate the SNR range of CoUEs.

In addition, some issues in detail need to be further discussed for the DS-RA scheme. On one hand, since each CoUE should establish uplink synchronization with one distributed TP at a time, for each CoUE, an access order, which is defined as an order of TPs that a CoUE establishes uplink synchronization with, should be arranged according to the intensity of the PLs from small to large. On the other hand, as stated in the signal model, different TPs are assumed to be allocated with different PRACH configuration indexes so that the RA signals of one TP have no impacts on others, which partly optimizes the performance of the DS-RA scheme.

B. Simulation Results

Case 1—Comparisons of the Proposed IPIC Algorithm With the Conventional Correlation Algorithm in RA Subchannels: Figs. 3–6 show the comparison of the proposed IPIC algorithm with the conventional correlation algorithm in terms of miss-detection (MD), power estimation, TO estimation, and complexity. To show the superiority of the IPIC algorithm and to select a proper maximum number of iterations, we assume that only one serving TP is utilized for multiuser detection, that the PL could be fully compensated, and that the retransmission and power ramping mechanisms are not employed. Without loss of generality, the RA subchannel for CoUEs is utilized for both

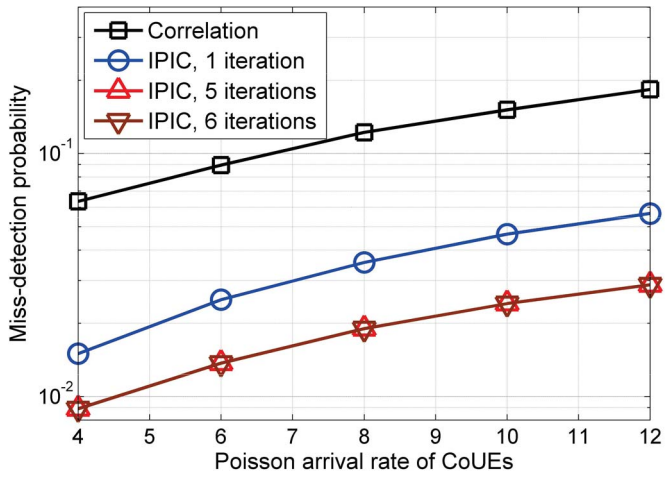

Fig. 3. MD performance with false-alarm rate kept around 1×10^{-3}.

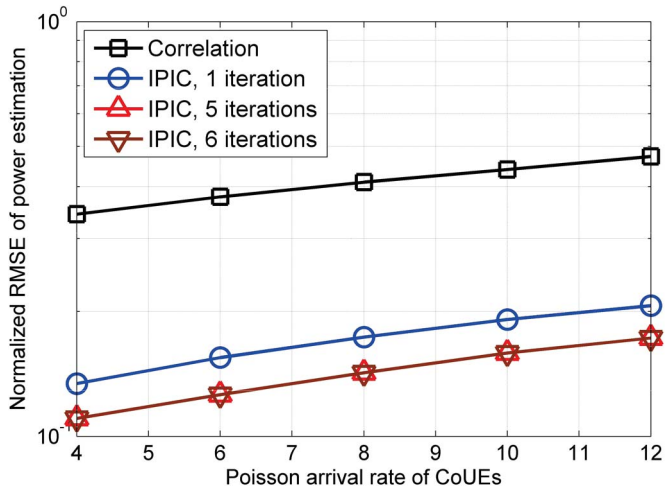

Fig. 4. Normalized RMSE of power estimation.

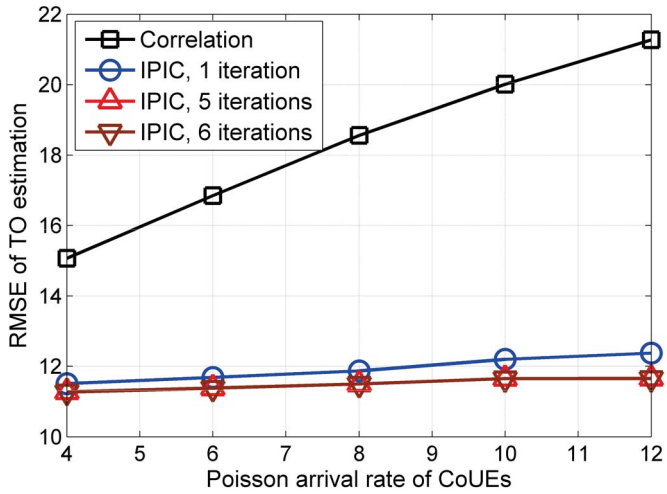

Fig. 5. RMSE of TO estimation.

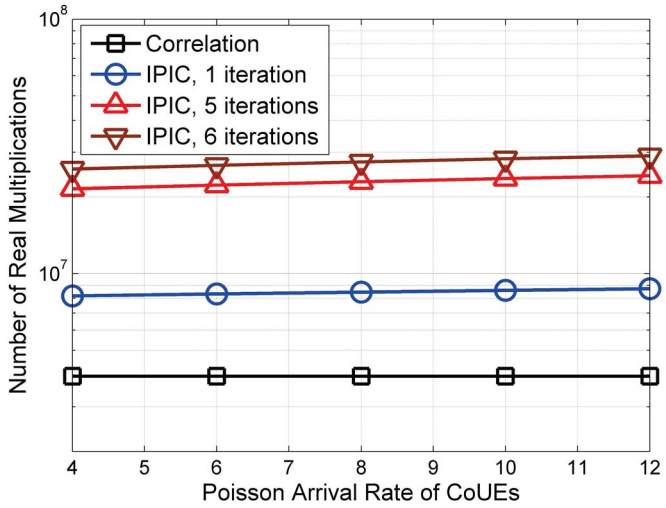

Fig. 6. Complexity of both algorithms.

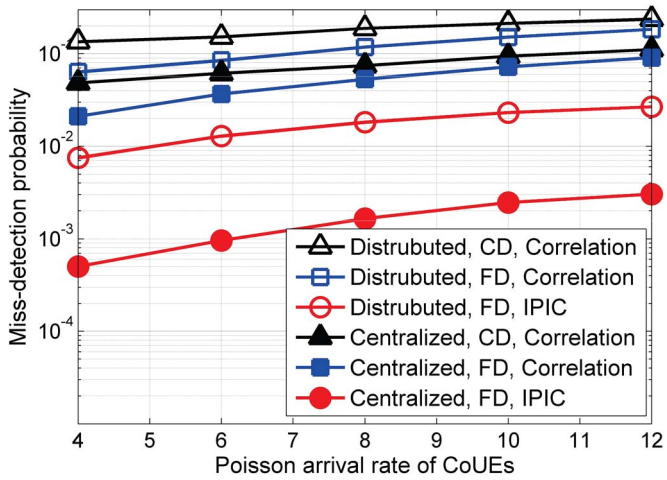

Fig. 7. MD performance with false-alarm rate kept around 1×10^{-3}.

algorithms with the Poisson arrival rate of CoUEs ranging from 4 to 12 per RA frame.

In Fig. 3, the MD performance of both algorithms is presented. The maximum number of iterations for the IPIC algorithm is set either $i_{\max} = 1,\ 5,$ or 6. It is shown that, with the number of iterations increasing from 1 to 5, there is an obvious increase in the MD performance, whereas no further increase is observed when the number of iterations increases from 5 to 6. This indicates that the IPIC achieves convergence at the fifth iteration. In addition, as expected, it is shown that the detection performance of the IPIC is significantly better than that of the correlation algorithm due to the reason that the proposed IPIC algorithm significantly mitigates the interference in each RA subchannel.

Figs. 4 and 5 show the normalized root MSE (RMSE) of power and TO estimation of both algorithms. When the number of iterations increases from 1 to 6, the estimation performance of the proposed IPIC also achieves convergence at the fifth iteration. It is shown that the normalized RMSE of power estimation of the IPIC algorithm is approximately 1/3 that of the correlation algorithm and that the RMSE of TO estimation of the IPIC algorithm is also 2–9 samples less than that of the correlation algorithm. The results indicate that the proposed IPIC algorithm could significantly improve the performance of power and TO estimation, facilitating the CU to perform initial TP clustering [11] and further CoMP transmission [3]–[5].

Fig. 6 shows the comparison of complexities of both algorithms. Because a real multiplication takes much more hardware resources than a real addition, we present the complexity by using the averaged number of real multiplications. For one thing, the complexity of the conventional algorithm keeps constant as it only performs one correlation processing for each possible code in the code set. For another, the complexity of the proposed IPIC is also robust to the number of CoUEs. This is because the complexity of the IPIC algorithm mainly comes from the correlation processing for all possible codes and is nearly proportional to the number of iterations, whereas the complexity for reconstructing the frequency signals of detected codes is almost negligible. When the number of iterations is 1, the complexity of the IPIC is approximately two times that of the conventional algorithm. When the number of iterations is 5, the complexity of the IPIC is approximately six times that of the conventional correlation algorithm.

By taking into account Figs. 3–6 together, in what follows, the number of iterations for the proposed IPIC is eventually selected as 5, which is actually a tradeoff between the performance and complexity. Compared with the correlation algorithm, with a few increase in the complexity, the proposed IPIC algorithm is able to significantly improve the RA performance in terms of multiuser detection and parameter estimation.

Case 2—Comparison of the Proposed RA Subchannel Allocation and Centralized Detection With Conventional PRACH: Fig. 7 shows the comparison of MD performance of both algorithms by utilizing the proposed RA subchannel for CoUEs and the conventional PRACH with distributed or centralized detection. In Fig. 7, "distributed" means distributed detection at distributed TPs and "centralized" means centralized detection at the CU by using three detection metrics from distributed TPs. "CD" stands for "code-division," representing the conventional PRACH with 839 RA subcarriers, and "FD" accounts for "frequency-division," representing the proposed RA subchannel for CoUEs with 409 RA subcarriers. To fairly compare the proposed RA subchannel with the conventional PRACH, both retransmission and power ramping mechanisms are not employed, and the PLs of CoUEs to all distributed TPs are perfectly compensated.

Inspection of Fig. 7 leads to the following conclusions. First, among all distributed detection schemes, the proposed IPIC algorithm in the proposed RA subchannel achieves the best detection performance. Second, the conventional correlation algorithm with the proposed RA subchannel achieves better MD performance than the conventional PRACH, which is in accordance with our analysis, indicating that the proposed RA subchannel is able to mitigate mutual interference between non-CoUEs and CoUEs. Finally, by comparing all centralized detection schemes with distributed schemes, as expected, it is shown that the coordinated diversity employed for centralized detection could significantly improve the MD performance.

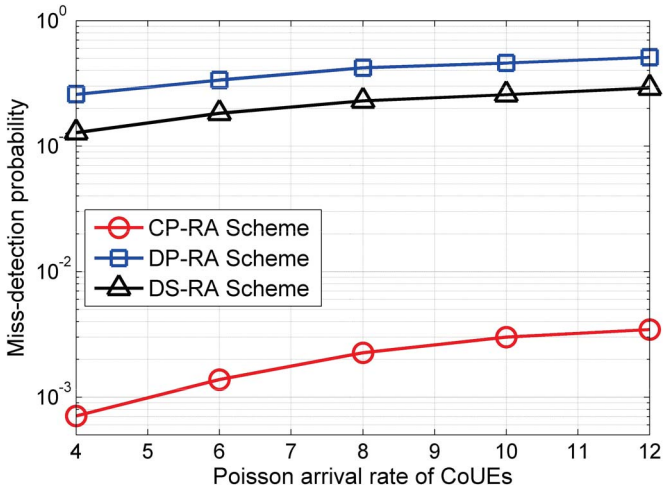

Fig. 8. MD performance with false-alarm rate kept around 1×10^{-3}.

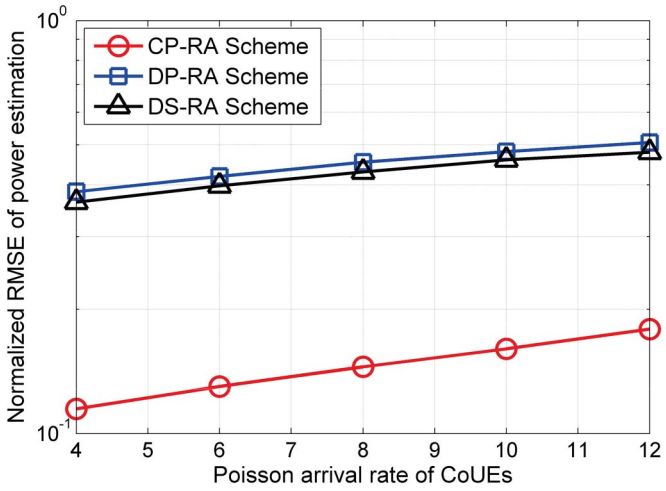

Fig. 9. Normalized RMSE of power estimation.

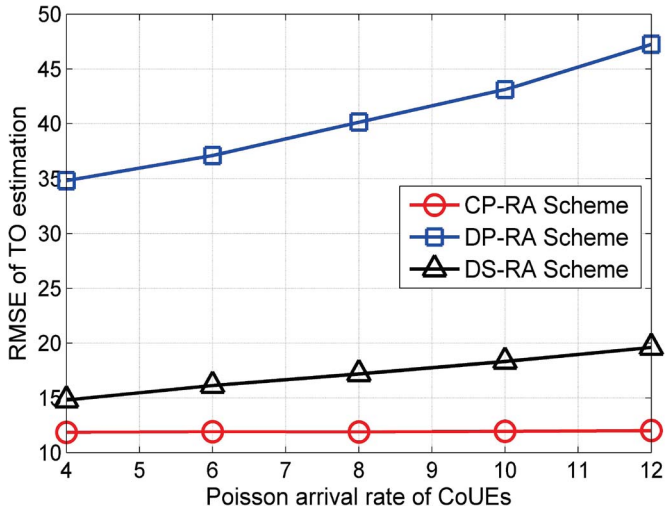

Fig. 10. RMSE of TO estimation.

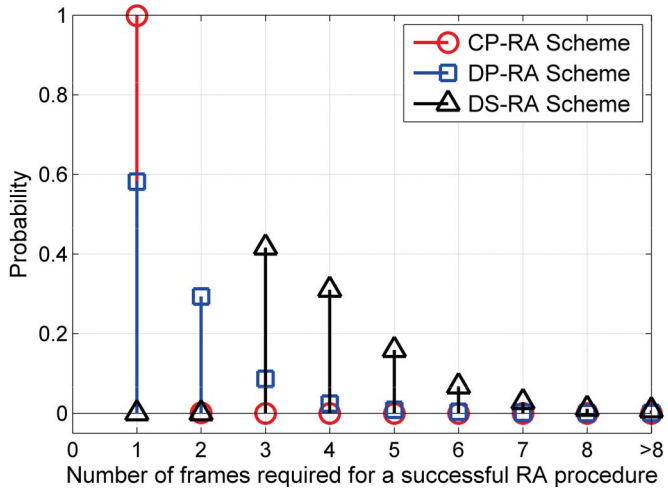

Fig. 11. Number of frames that are required for a successful RA procedure with the Poisson arrival rate of CoUEs being 6.

Note that the correlation algorithm in the conventional PRACH with centralized detection is performed just for comparison purpose as it is hard for the CU to distinguish code-division multiplexed CoUEs from non-CoUEs. All of these indicate that the proposed RA subchannel allocation and centralized detection are of great effectiveness to improve the detection performance for both CoUEs and non-CoUEs.

Case 3—Comparisons of CP-RA With DP-RA and DS-RA: Figs. 8–11 show the comparison of the proposed CP-RA scheme with the DP-RA and DS-RA schemes in terms of multiuser detection, power estimation, TO estimation, and access delays. To completely compare these RA schemes, both resubmission and power ramping mechanisms are employed for failed CoUEs. If a UE fails to complete the current RA process, its transmitting power is gradually increased for the next RA procedure unless the maximum transmitting power is achieved, and the maximum transmitting power holds until a maximum retry time (i.e., eight RA frames) is reached.

Figs. 8–10 show the comparison of detection and estimation performance of three RA schemes. It is obviously observed that the detection performance of the proposed CP-RA scheme outperforms that of both DP-RA and DS-RA schemes and that the CP-RA scheme performs better power and TO estimation performance than the DP-RA and DS-RA schemes. Furthermore, two more phenomena could be observed. On one hand, it is shown that the DS-RA scheme outperforms the DP-RA scheme, which can be explained in twofold. 1) With a fixed initial number of CoUEs, signals of CoUEs should be simultaneously processed by all distributed TPs in parallel RA schemes, whereas signals of CoUEs are separately processed by their respective TPs in the DS-RA scheme, indicating that the DS-RA scheme is supposed to suffer less interference than parallel RA schemes. 2) In parallel RA schemes, as the transmitting power of a CoUE is adjusted according to the minimum PL of one TP to alleviate the NFE, the transmitting power of a CoUE cannot reach the target receiving power for other TPs, which also inversely impacts the detection performance of parallel RA schemes. On the other hand, noting that the CP-RA scheme relates to the centralized IPIC-based detection and that the DP-RA scheme relates to the distributed

correlation-based detection in the conventional PRACH in Fig. 7, it can be observed that both parallel RA schemes become worse compared with that in Fig. 7 because 1) the PLs of CoUEs may not be fully compensated in parallel RA schemes as previously stated, and 2) the employment of resubmission results in accumulation of failed CoUEs for further RA frames, leading to larger MAI than that in Fig. 7. The previous analyses indicate that the performance of parallel RA schemes strongly depends on the effectiveness of the multiuser detection and estimation algorithm. Benefiting from the proposed IPIC algorithm, the proposed CP-RA scheme is able to significantly improve the RA performance compared with the DP-RA scheme.

Fig. 11 shows the number of RA frames that is required for a successful RA procedure. It is shown that the CP-RA scheme requires one RA frame to complete the RA procedure at the probability of 0.99, whereas the DP-RA scheme at the probability of 0.57, meaning that the CP-RA scheme could provide better RA efficiency than the DP-RA scheme. On the other hand, as the DS-RA scheme necessitates at least three RA frames to complete the RA procedure, it offers the worst RA efficiency. By taking into account the simulation results in Figs. 8–11 together, we can come to a final conclusion that the proposed CP-RA scheme is able to provide significantly better RA performance and efficiency than the available DP-RA and DS-RA schemes for the CoMP transmission.

V. Conclusion

In this paper, a CP-RA scheme has been proposed for the CoMP transmission in LTE systems. By utilizing the proposed scheme, the CU is able to obtain the knowledge about power and TOs from CoUEs to distributed TPs for further CoMP transmission. Consisting of a novel RA subchannel allocation scheme, an IPIC-based multiuser detection and estimation algorithm, and a centralized detection scheme exploiting coordinated diversity, the CP-RA scheme could suppress mutual interference between CoUEs and non-CoUEs and significantly improve the multiuser detection and estimation performance. Analyses and simulation results show that the CP-RA scheme is able to offer improved RA performance with a few increase in complexity, and the extra complexity is paid off to improve user experience and system efficiency.

Appendix
Conventional Correlation-Based Algorithm

By treating other active codes as interference, the correlation-based algorithm is proceeded for each possible code $\mathbf{C}_v$, and an M-point IDFT is utilized to obtain the LS estimation of the transform-domain channel taps, i.e.,

$$\begin{aligned}\widehat{\boldsymbol{g}}_v^{(b)} &= \left[\widehat{g}_{v_k}^{(b)}(0),\ldots,\widehat{g}_{v_k}^{(b)}(\ell),\ldots,\widehat{g}_{v_k}^{(b)}(M-1)\right]^T \\ &= \frac{1}{M}\mathbf{Q}^H\mathbf{C}_v^H\mathbf{Y}^{(b)}. \end{aligned} \tag{33}$$

As the ZC codes are actually generated as cyclic-shift versions of one root ZC sequence in the transform domain before DFT precoding, defining the length of cyclic shift of ZC codes as $N_{\rm cs}$, if $\ell \geq N_{\rm cs}$, the current ZC code becomes another one, indicating that only the channel estimates with indexes $\ell \in [0, N_{\rm cs}-1]$ could be utilized. The variance of interference is then estimated as

$$\widehat{\sigma}_v^{(b)2} = \frac{1}{N_{\rm cs}-D_{\max}-1}\sum_{\ell=D_{\max}+1}^{N_{\rm cs}-1}\left|\widehat{g}_v^{(b)}(\ell)\right|^2 \tag{34}$$

where $d_{\max}$ is the maximum TO of all active UEs, and $D_{\max} = \lceil (d_{\max}+L-1)M/N\rceil < N_{\rm cs}-1$ is defined as the maximum delay spread of the transform-domain channel taps corresponding to that of the time-domain channel taps with a scaler factor M/N according to the SC-FDMA structure [19].

For the current code, the detection metric and estimates of the TO and power are then determined as

$$\Upsilon_v^{(b)} = \max_{\ell\in[0,D_{\max}]}\frac{1}{\widehat{\sigma}_v^{(b)}}\left|\widehat{g}_v^{(b)}(\ell)\right| \tag{35}$$

$$\widehat{d}_v^{(b)} = \frac{N}{M}\cdot\arg\max_{\ell\in[0,D_{\max}]}\frac{1}{\widehat{\sigma}_v^{(b)}}\left|\widehat{g}_v^{(b)}(\ell)\right| \tag{36}$$

$$\widehat{P}_v^{(b)} = \left|\widehat{g}_v^{(b)}\left(\widehat{d}_v^{(b)}\right)\right|^2. \tag{37}$$

If $\Upsilon_v^{(b)} > \lambda$, where λ is a predefined threshold, the current code is active with its estimation results given in (36) and (37). Otherwise, it is deemed inactive.

References

[1] J. Lee *et al.*, "Coordinated multipoint transmission and reception in LTE-Advanced systems," *IEEE Commun. Mag.*, vol. 50, no. 11, pp. 44–50, Nov. 2012.

[2] M. Sawahashi, Y. Kishiyama, A. Morimoto, D. Nishikawa, and M. Tanno, "Coordinated multipoint transmission/reception techniques for LTE-Advanced: Coordinated and distributed MIMO," *IEEE Wireless Commun.*, vol. 17, no. 3, pp. 26–34, Jun. 2010.

[3] L. Zhao, K. Liang, G. Cao, R. Qian, and D. Lopez-Perez, "An enhanced signal-timing-offset compensation algorithm for coordinated multipoint-to-multiuser systems," *IEEE Commun. Lett.*, vol. 18, no. 6, pp. 983–986, Jun. 2014.

[4] S. Iwelski *et al.*, "Feedback generation for CoMP transmission in unsynchronized networks with timing offset," *IEEE Commun. Lett.*, vol. 18, no. 5, pp. 725–728, May 2014.

[5] V. Kotzsch, W. Rave, and G. Fettweis, "Interference cancellation and suppression in asynchronous cooperating base station systems," in *Proc. Int. ITG Workshop Smart Antennas*, Mar. 2012, pp. 78–85.

[6] T. Koivisto, T. Kuosmanen, and T. Roman, "Estimation of time and frequency offsets in LTE coordinated multi-point transmission," in *Proc. IEEE 78th VTC*, Sep. 2013, pp. 1–5.

[7] S. Kim, K. Joo, and Y. Lim, "A delay-robust random access preamble detection algorithm for LTE systems," in *Proc. IEEE RWS*, Jan. 2012, pp. 75–78.

[8] Y. Hu *et al.*, "A method of PRACH detection threshold setting in LTE TDD femtocell system," in *Proc. 7th Int. Conf. Commun. Netw. China*, Aug. 2012, pp. 408–413.

[9] X. Yang and A. O. Fapojuwo, "Enhanced preamble detection for PRACH in LTE," in *Proc. IEEE WCNC*, Apr. 2013, pp. 3306–3311.

[10] B. Liang, Z. He, K. Niu, B. Tian, and S. Sun, "The research on random access signal detection algorithm in LTE systems," in *Proc. IEEE 5th Int. Symp. MAPE*, Oct. 2013, pp. 115–118.

[11] C. Yang, S. Han, X. Hou, and A. F. Molisch, "How do we design CoMP to achieve its promised potential," *IEEE Wireless Commun.*, vol. 20, no. 1, pp. 67–74, Feb. 2013.

[12] "Evolved Universal Terrestrial Radio Access (E-UTRA), carrier aggregation, base station radio transmission and reception," Third-Generation Partnership Project, Sophia Antipolis, France, Tech. Rep. 36.808 v.10.1.0, Jul. 2013.

[13] D. H. Lee and H. Morikawa, "Random access transmit power control algorithm of LTE system in relay network," in *Proc. 20th Int. Symp. Pers., Indoor, Mobile Radio Commun.*, Sep. 2009, pp. 905–909.
[14] J. Fessler and A. Hero, "Space-alternating generalized expectation–maximization algorithm," *IEEE Trans. Signal Process.*, vol. 42, no. 10, pp. 2664–2677, Oct. 1994.
[15] "Evolved Universal Terrestrial Radio Access (E-UTRA): User Equipment Radio Transmission and Reception," Third-Generation Partnership Project, Sophia Antipolis, France, Tech. Specification 36.211, v.11.4.0, Sep. 2013.
[16] "Evolved Universal Terrestrial Radio Access (E-UTRA): Medium Access Control (MAC) Protocol Specification," Third-Generation Partnership Project, Sophia Antipolis, France, Tech. Specification 36.321, v.12.1.0, Mar. 2014.
[17] K. Larsson, J. Christoffersson, A. Simonsson, B. Hagerman, and P. Cosimini, "LTE outdoor & indoor interference assessment based on UE measurements," in *Proc. IEEE Conf. Veh. Technol.*, May 2011, pp. 1–5.
[18] N. Kabaoglu, "SAGE based suboptimal receiver for downlink MC-CDMA system," *IEEE Commun. Lett.*, vol. 15, no. 12, pp. 1381–1383, Dec. 2011.
[19] D. D. Falconer, "Linear precoding of OFDMA signals to minimize their instantaneous power variance," *IEEE Trans. Commun.*, vol. 59, no. 4, pp. 1154–1162, Apr. 2011.
[20] Y. Zhou, Z. Hou, Z. Pan, J. Shi, and J. Wang, "Dynamic Doppler tracking for LTE-based broadband communications on high speed rails," in *Proc. IEEE Int. Conf. ChianSIP*, Jul. 2013, pp. 389–393.
[21] D. Lee *et al.*, "Coordinated multipoint transmission and reception in LTE-Advanced: Deployment scenarios and operational challenges," *IEEE Commun. Mag.*, vol. 50, no. 2, pp. 148–155, Feb. 2012.
[22] "Coordinated multi-point operation for LTE physical layer aspects," Third-Generation Partnership Project, Sophia Antipolis, France, Tech. Specification 36.819, v.11.2.0, Sep. 2013.

Qiwei Wang was born in Henan, China, in 1987. He received the B.S. degree in communication engineering from Harbin University of Science and Technology, Harbin, China, in 2009, and the M.S. degree in communication and information systems from Xidian University, Xi'an, China, in 2012, where he is currently working toward the Ph.D. degree in communication and information systems.

His current research interests include uplink synchronization in orthogonal frequency-division multiple-access systems, including the initial ranging process in WiMAX systems, the random access procedure in Long-Term Evolution (LTE) systems, multiuser detection and parameter estimation, and coordinated multipoint.

Guangliang Ren (M'06) was born in Jiangsu, China, in 1971. He received the B.S. degree in communication engineering from Xidian University, Xi'an, China, in 1993; the M.S. degree in signal processing from Ordnance Science and Research Academy of China, Beijing, China, in 1996; and the Ph.D. degree in communication and information systems from Xidian University in 2006.

He is currently a Professor with the School of Telecommunications Engineering, Xidian University. He is the author of more than 40 research papers in journals and conference proceedings, such as the IEEE TRANSACTIONS ON COMMUNICATIONS, the IEEE TRANSACTIONS ON WIRELESS COMMUNICATIONS, and the IEEE TRANSACTIONS ON VEHICULAR TECHNOLOGY, and an author or coauthor of three books. His research interests include wireless communication and digital signal processing, particularly multiple-input–multiple-output systems, WiMAX, and Long-Term Evolution (LTE).

Jueying Wu was born in Guangxi, China, in 1991. She received the B.S. degree in communication engineering from Xidian University, Xi'an, China, in 2013, where she is currently working toward the M.S. degree in communication and information systems.

Her current research interests include uplink synchronization in orthogonal frequency-division multiple-access systems, including the random access procedure in Long-Term Evolution (LTE) systems, multiuser detection and parameter estimation, and coordinated multipoint.